Serial electron microscopic reconstruction of the *drosophila* larval eye: Photoreceptors with a rudimentary rhabdomere of microvillar-like processes

Volker Hartenstein [a,*], Michaela Yuan [b], Amelia Younossi-Hartenstein [a], Aanavi Karandikar [a], F. Javier Bernardo-Garcia [c], Simon Sprecher [c], Elisabeth Knust [b]

[a] *Department of Molecular Cell and Developmental Biology, University of California Los Angeles, Los Angeles, CA, 90095, USA*
[b] *Max-Planck-Institute of Molecular Cell Biology and Genetics, Pfotenhauerstr. 108, 01307, Dresden, Germany*
[c] *Department of Biology, University of Fribourg, 10, Ch. du Musée, 1700, Fribourg, Switzerland*

A R T I C L E   I N F O

A B S T R A C T

Photoreceptor cells (PRCs) across the animal kingdom are characterized by a stacking of apical membranes to accommodate the high abundance of photopigment. In arthropods and many other invertebrate phyla PRC membrane stacks adopt the shape of densely packed microvilli that form a structure called rhabdomere. PRCs and surrounding accessory cells, including pigment cells and lens-forming cells, are grouped in stereotyped units, the ommatidia. In larvae of holometabolan insects, eyes (called stemmata) are reduced in terms of number and composition of ommatidia. The stemma of *Drosophila* (Bolwig organ) is reduced to a bilateral cluster of subepidermal PRCs, lacking all other cell types. In the present paper we have analyzed the development and fine structure of the *Drosophila* larval PRCs. Shortly after their appearance in the embryonic head ectoderm, PRC precursors delaminate and lose expression of apical markers of epithelial cells, including Crumbs and several centrosome-associated proteins. In the early first instar larva, PRCs show an expanded, irregularly shaped apical surface that is folded into multiple horizontal microvillar-like processes (MLPs). Apical PRC membranes and MLPs are covered with a layer of extracellular matrix. MLPs are predominantly aligned along an axis that extends ventro-anteriorly to dorso-posteriorly, but vary in length, diameter, and spacing. Individual MLPs present a "beaded" shape, with thick segments (0.2–0.3 μm diameter) alternating with thin segments (>0.1 μm). We show that loss of the glycoprotein Chaoptin, which is absolutely essential for rhabdomere formation in the adult PRCs, does not lead to severe abnormalities in larval PRCs.

1. Introduction

Metazoan photoreceptors carry light-sensitive, G-protein coupled receptors (opsins) in their membrane that activate a phototransduction cascade resulting in a receptor potential. The small integration time and high detection accuracy of photic changes that are required for photoreceptors to control even simple visual tasks demand large numbers of opsin proteins to be packed into the cell, which in turn requires an increase in surface area achieved by membrane stacking (Nilsson, 2013). This process exploits the naturally occurring membrane specializations of prototypical epithelial cells from which photoreceptors evolved, cilia and microvilli. Photoreceptors of the ciliary type possess specialized cilia, which increase surface area by invaginating their membrane (e.g., discs of vertebrate rods and cones; tubules of chaethognath photoreceptors) or extending membrane folds to the outside (lamellae or villi in photoreceptors of ctenophores, cnidaria, echinoderms and cephalochordates; reviewed in (Eakin, 1965; Lacalli, 2004; Randel and Jékely, 2016, Fig. 1). Alternatively, membrane stacking occurs by the increase in number, size and packing density of microvilli, which are organized into prominent arrays called rhabdomeres. Rhabdomeric photoreceptors also occur in multiple types. For example, in the simple cup eyes of platyhelminths and many other protostomes, they form tufts of apically directed microvilli, or elongated, more irregularly oriented villi and "microvillar-like" processes (Eakin, 1965, 1972; Arendt, 2003; Purschke et al., 2006, Fig. 1). In

* Corresponding author. Department of Molecular, Cell, and Developmental Biology, University of California Los Angeles, 610 Charles E. Young Drive, 5014 Terasaki Life Sciences Bldg, Los Angeles, CA, 90095-1606, USA.
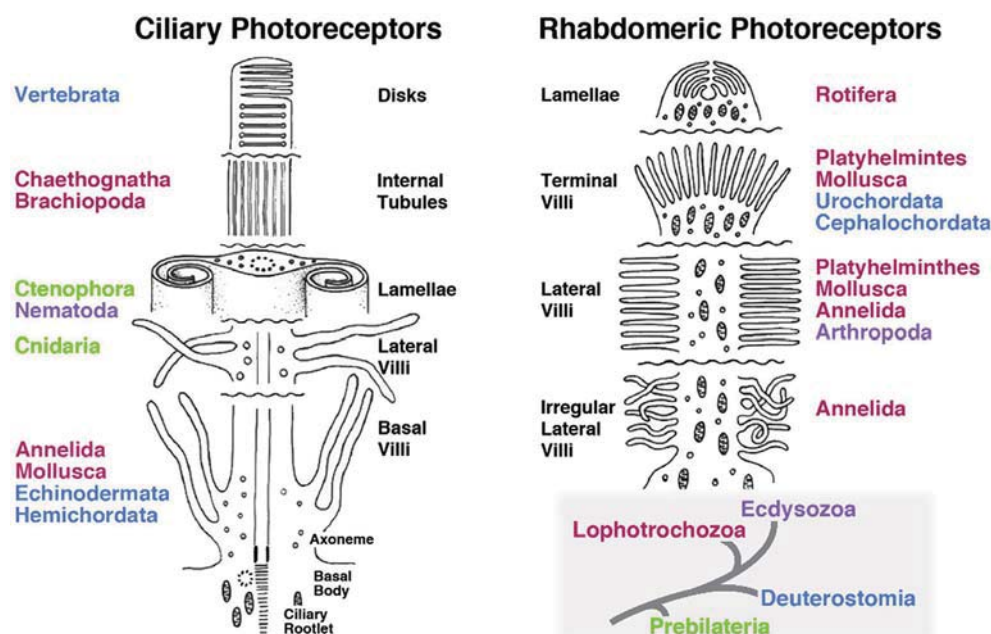*E-mail address:* volkerh@mcdb.ucla.edu (V. Hartenstein).

Fig. 1. Schematic "totempole" view of different modes of membrane stacking occurring in ciliary and rhabdomeric photoreceptors (modified from (Eakin, 1965), with permission). Names of animal clades for which given mode is observed are rendered in colors that represent the superphyla prebilateria (Ctenophora, Cnidaria; green), Lophotrochozoa (red), Ecdysozoa (purple), Deuterostomia (blue; see bottom right).

the complex eyes of arthropods, which are capable of high-resolution vision, the apical membrane of photoreceptors is typically tilted sideways, resulting in a large rhabdomere of perfectly parallel, horizontally directed microvilli.

Recent molecular and physiological studies of opsin receptors and phototransduction processes showed that the structurally based definition of ciliary and rhabdomeric photoreceptors is coupled with fundamental functional differences between these two types of cells. Ciliary photoreceptors possess c-opsins which activate the Gi/t-mediated cGMP cascade that results in a negative (hyperpolarizing) receptor potential, whereas rhabdomeric receptors produce a positive (depolarizing) potential mediated via r-opsins that activate the Gq-mediated IP3 cascade (Fain et al., 2010; Fernald, 2006; Gehring, 2014). The picture that emerges indicates that both types appeared early in metazoan evolution and were present in the bilaterian ancestor, or even bilaterian-cnidarian, ancestor, and then evolved in parallel to give rise to the multiple ciliary and rhabdomeric photoreceptors encountered today.

Despite of the long evolutionary time period that separates ciliary and rhabdomeric photoreceptors, molecular mechanisms controlling their morphogenesis appear to be highly conserved. Best understood among these is the pathway that involves the Crumbs (Crb) protein complex. Factors of this complex, which control the polarity of epithelial (and other) cells in general, were coopted to shape the apical membrane specializations of photoreceptors (Ready and Tepass, 2004; Richard et al., 2006; Knust, 2007). In *Drosophila*, the apically located Crb-complex specifies the size of the stalk membrane, a portion of the apical mebrane localized between the rhabdomere and the *zonula adherens*. In addition, Crb is also involved in the transport of opsin into the rhabdomeric microvilli (Pocha et al., 2011). Impaired function of Crb in *Drosophila* and mammals alike result in morphogenetic defects of photoreceptor cells; in human, mutations of the Crb1 gene are the underlying cause of degenerative diseases like retinitis pigmentosa 12 (RP12) and Leber congenital amaurosis (Richard et al., 2006; Quinn et al., 2017). Strikingly, *Drosophila* PRCs lacking Crb undergo light-dependent retinal degeneration (Johnson et al., 2002). To exert their effect on rhabdomeric or ciliary structure, proteins of the Crb complex must interact in multiple ways with components of the apical membrane-associated cytoskeleton of the developing photoreceptors. Studies in tractable genetic model systems

that uncover these interactions will be instrumental to understand how photoreceptors evolve ontogenetically and phylogenetically, and to develop approaches to treat many human eye diseases. Genetic studies in *Drosophila* have focused for the most part on the formation of the adult compound eye which differentiates during metamorphosis from the eye imaginal disc (Charlton-Perkins and Cook, 2010; Treisman, 2013). By contrast, little is known about the larval eye, or Bolwig organ (BO), which consists of a small group of photoreceptors that differentiate in the embryo, and steer phototactic and photoperiodic behaviors of the larva (Keene and Sprecher, 2012). In the present paper we have reconstructed the ultrastructure of the BO using serial transmission electron microscopy, and addressed aspects of BO development that pertain to photoreceptor polarity.

Larval eyes, or stemmata, are ubiquitously found in holometabolan insects. As opposed to the compound adult eyes, which are large, modular arrays of small groups of photoreceptors (ommatidia) shielded by a pigment cell layer, stemmata are simpler eyes comprised of single or small groups of ommatidia; in many cases, these ommatidia are fused together into larger complexes of tens to hundreds of receptor cells joined together in a single photosensitive epithelium capped by a lens ("fusionsstemma"; (Melzer and Paulus, 1989). It has been proposed that stemmata are homologous to the posterior-most ommatidia of primitive (hemimetabolous) insects (Melzer and Paulus, 1989; Paulus, 1989; Friedrich, 2003, 2011; Liu and Friedrich, 2004; Buschbeck, 2014). In these, a dorsal domain of the embryonic head ectoderm becomes specified as the eye field, from which photoreceptors and other retinal cell types develop in a posterior to anterior temporal gradient (Friedrich, 2003). It has been proposed that such a posterior to anterior wave of eye specification is also triggered in embryos of holometabolans. However, the wave comes to a halt after the first (posterior) groups of cells have adopted the fate of eye cells. These cells subsequently assemble into the larval stemmata. The remainder of the eye field remains undifferentiated throughout the larval period during which it exists as a proliferating eye primordium. The eye primordium then re-commences development with the onset of metamorphosis to give rise to the adult compound eye (Friedrich, 2003).

In higher dipterans (Cyclorrhapha) the modifications that separate larval photoreceptors from the canonical rhabdomeric cells found in

adult compound eyes go several steps further. Lense and pigment forming cells are absent, and photoreceptor cells have lost their rhabdomeres (Melzer and Paulus, 1989). Larvae of these flies have involuted their head structures into the body interior, with the result that many sensory organs, including the larval eye [called "Bolwig organ" (BO)], have disappeared from the surface and are anchored to an epithelial fold (dorsal pouch) that surrounds the pharynx (Bolwig, 1946; Steller et al., 1987; Hartenstein, 1988; Green et al., 1993; Melzer and Paulus, 1989, Fig. 2A). During the process of head involution, precursors of the BO photoreceptors completely separate from the ectoderm and lose their epithelial phenotype. Consecutively, PRCs undergo a rotation, so that their original apical pole now faces away from the epithelium that gave rise to these cells (Fig. 2A). Instead of the regularly stacked microvilli typical for rhabdomeres, the outer (former apical) membrane of larval PRCs is drawn into elongated processes, called "lamellae" by Melzer and Paulus (1989) and Green et al. (1993) who provide descriptions of representative electron microscopic sections of the BO of late third instar larvae. The same phenotype was described for the larval eyes of Muscidae (Melzer and Paulus, 1989).

Drosophila larval vision, mediated by the BO, has been the focus of several recent functional studies, including (Essen et al., 2011; Humberg et al., 2018; Humberg and Sprecher, 2017; Justice et al., 2012; Kane et al., 2013; Keene et al., 2011). The BO, due to its simplicity in terms of cell types and rapid development during the embryonic period, has also a

rich source for developmental genetic analysis (Sprecher et al., 2007; Sprecher and Desplan, 2008; Vasiliauskas et al., 2011; Mishra et al., 2013, 2016; Zhou et al., 2017). To further aid in these studies a more detailed understanding of the ultrastructural details of the BO photoreceptor membrane specializations is required. Since the three-dimensional architecture of subcellular structures like the "lamellae" can only be captured in serial electron microscopy, we generated a complete series of more than 300 consecutive cross sections of a first instar larval BO and processed these sections for a 3D digital reconstruction using the TrakEM2 software package (Cardona et al., 2012). In addition, we investigated the expression of apical proteins [Crb, Armadillo/b-catenin, Pericentrin-like Protein (PLP), Asterless (Asl); Pellikka et al., 2002; Johnson et al., 2002; Izaddoost et al., 2002; Fan, 2004; Martinez-Campos et al., 2004; Novak et al., 2014] known to be important in controlling polarity and differentiation of canonical photoreceptors and/or sensory ciliary structures.

Our results demonstrate that precursors of the larval PRCs strongly downregulate or lose the expression of apical markers as they delaminate from the embryonic head ectoderm. Confirming our previous analysis (Green et al., 1993), we show that differentiated PRCs have changed in orientations so that their former apical pole faces basally, away from the epithelium from which they have delaminated earlier. Whereas adult PRCs are characterized by a constricted apical membrane, divided into a narrow central rhabdomere and flanking stalk, larval PRCs have an
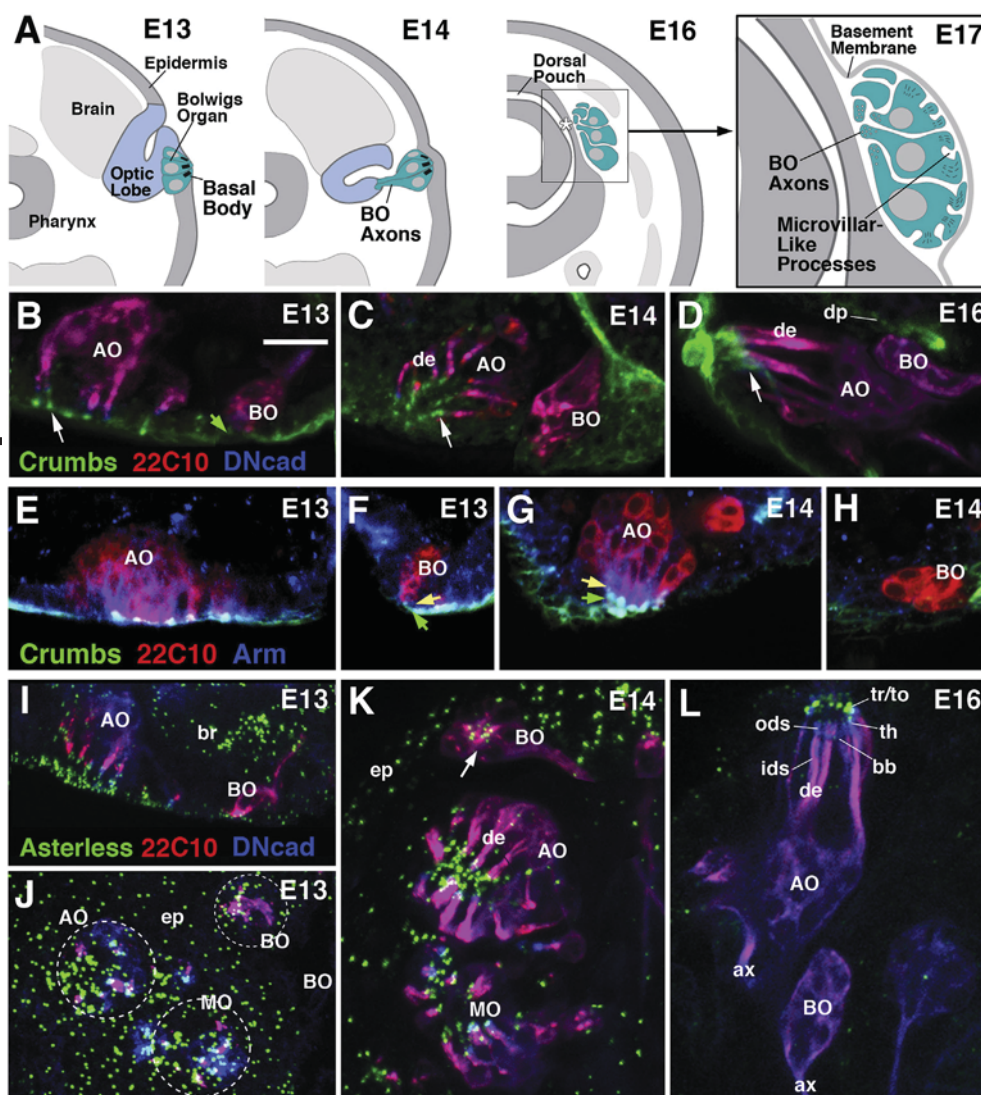
Fig. 2. Embryonic development of BO photoreceptors. (A) Schematic representations of cross sections of the right half of the head region of an embryo at stages 13, 14, 16, and 17. (B–L) Z-projections of horizontal confocal sections (B, D-I, L) and parasagittal (C, J, K) of embryonic head. (B–D) Labeling with anti-Crumbs (Crb, green), anti-Futsch (22C10, red) and anti-DN-cadherin (DNcad, blue). Note global Crb staining along apical membranes of ectoderm, including BO PRC precursors (green arrow) in (B). Crb-expression is upregulated in developing inner segments of sensory neurons of the antennal organ (AO, white arrow in B-D), but disappears from precursors of Bolwig organ (BO) after stage 14 (C, D). (E–H) Labeling with anti-Crumbs (green), anti-Futsch (red), and anti-Armadillo/β-catenin (Arm, blue), which is concentrated in subapical membrane around the *zonula adherens* (yellow arrow in F, G). Expression of Crb (green arrow) and Arm (yellow arrow) remains high in sensory neurons of antennal organ (AO in panel G) but disappears from Bolwig organ (H). (I–L) Labeling with anti-Asterless (green), anti-Futsch (red) and anti-DN-cadherin (blue). Asterless marks the centrioles which give rise to the basal body located in the inner dendritic segment of sensory neurons. Note ubiquitous centriolar staining at stage 13 (I, J). Staining is still visible in BO photoreceptor precursors at stage 14, but has disappeared from these cells by stage 16 (L). By contrast, strong labeling in cells of the antennal organ (AO) marks the basal bodies (bb) at the junction of inner (ids) and outer (ods) dendritic segments, as well centrioles associated with the support cells of the neurons (th thecogen cell, to/tr tormogen/trichogen cell). Other abbreviations: ax axon; br brain; de dendrite; dp dorsal pouch; ep epidermis; MO maxillary organ. Bar: 10 μm (B–L).

3

expanded, irregularly shaped apical surface which is folded into multiple horizontal microvillar-like processes (MLPs). Most MLPs are roughly aligned along an axis that extends ventro-anteriorly to dorso-posteriorly relative to the body axis. However, in contrast to the extremely regular, "crystalline" size/shape and positioning of microvilli forming the adult rhabdomeres, larval MLPs vary in length, diameter, and spacing. Our serial reconstruction showed that individual MLPs present a peculiar "beaded" shape, whereby short, thick segments of 0.2–0.3 μm diameter alternate with thin segments measuring <0.1 μm. Finally, we show that loss of the glycoprotein Chaoptin, which is absolutely essential for rhabdomere formation in the adult PRCs (Reinke et al., 1988); (Van Vactor et al., 1988), does not lead to severe abnormalities in PRCs of the larval Bolwig organ. Our data provide support for future functional and developmental studies of this simplified and miniaturized eye with its highly modified rhabdomeric structure.

2. Material and methods

2.1. Fly lines

γ-tubulin 37C-GFP (Bloomington #56831) was used to detect γ-tubulin. The wild-type line y^{1118} (Bloomington #5905) was utilized for the immunohistochemical labeling experiments. Rh5-Gal4 (Mollereau et al., 2000) and *UAS-mCD8::RFP* (Bloomington #32219) were used to study the expression of the Rh5 in the BO.

2.2. Antibodies

We used rat anti-*Drosophila* N-Cadherin (1:10) and mouse anti-Futsch (22C10; 1:10) (Developmental Studies Hybridoma Bank). Other primary antibodies included rabbit anti-Plp (Martinez-Campos et al., 2004; 1:500), rabbit anti-Asl (Varmark et al., 2007; Novak et al., 2014; 1:500) (both antibodies generously gifted by Dr. J. Raff), mouse anti-Rh6 (Chou et al., 1999; 1:40; generously gifted by Dr. S. Britt), and rabbit anti-DsRed (1:100, Clontech # 632496). Secondary antibodies were anti-Rabbit Cy-3 (1:330) (Jackson ImmunoResearch), anti-Mouse Alexa Fluor 488 (1:1000) (Life Technologies), and anti-Rat Cy-5 (1:500) (Jackson Immu-noResearch), and anti-Mouse Cy-3 (1:300) (Jackson ImmunoResearch).

2.3. Embryo collection

Adult *Drosophila* were placed in an egg laying chamber containing a grape juice agar plate. Several drops of a yeast mixture were added to the plate, and the egg laying chamber was kept at 25 °C. Following a 24 h collection period embryos were washed off of the grape juice plate. The chorion membranes were stripped off by treating the sample with bleach (15min) and rinsed with ddH20.

2.4. Immunohistochemistry

Washed embryos without chorion membranes were transferred to a 1.5 ML Eppendorf tube with 600 μL of heptane. A fixative solution of 375 μL PEMS and 125 μL of 16% paraformaldehyde (PFH) was added to the heptane (40 min at room temperature). The clear aqueous bottom layer was removed, and 500 μL of 100% methanol (MeOH) was added to devitellinize the embryos. The tube was rapidly shaken until most of the embryos fell to the bottom. The MeOH was removed, and the sample was rinsed two additional times with 500 μL of 100% MeOH (10 min). The sample was then rehydrated by adding 300 μL of 100% MeOH and 0% PBS (10 min), then 300 μL of 75% MeOH and 25% PBS (15 min). The procedure was repeated with 300 μL of 50% MeOH and 50% PBS (20 min), then 300 μL of 25% MeOH and 75% PBS. The sample was then rinsed in PBT (just by inverting the tube) then washed in PBT for 40 min. It was then blocked in 300 μL of a 9 parts PBT, 1 part Normal Goat Serum solution (PBT + N) for 30 min. The primary antibodies were added, and the sample was incubated at 4 °C for 2 days. Embryos were then washed

in PBT (2 × 20 min), blocked in PBT + N (30 min), and incubated in the secondary antibodies for 2 days.

2.5. Confocal imaging

After incubating the sample in secondary antibodies, it was rinsed in PBT (3x just invert), and then washed in PBT (20 min). Samples were mounted in VECTASHIELD, and then imaged using a Zeiss LSM700. Images were stored and analyzed using the Fiji/ImageJ software package (https://fiji.sc/). We analyzed at least five embryos for a given stage, from stage 12–16, and marker combination. Preparations were recorded in dorsal and lateral orientation.

2.6. Digital reconstruction and analysis of SU neurons from serial EM

Photoreceptors of the larval eye neurons were reconstructed from a series of 324 TEM sections of the head of one first instar larva. The region section contained more than 90% of the BO, with only the anterior and posterior tip missing. Tissue was fixed by high pressure freezing (Leica EM Pact 2) and freeze substitution (Leica EM AFS 2), using a solution of 1% osmiumtetroxide and 0.1% uranyl acetate in acetone. Sections of 60–80 nm were cut on a Leica Ultracut UCT and poststained in a 2% uranylacetate/lead citrate solution. Grids were imaged with a Tecnai 12 Biotwin TEM, using a fast-scan F214A CCD camera controlled by the SerialEM software (Boulder Lab). The digital image stack was imported into the TrakEM2 package (Cardona et al., 2012) which manages tiling and registration of images, as well as subsequent steps of segmentation and 3D rendering. We segmented by painting processes as "area lists", using the tool provided by the TrakEM2 software.

3. Results

3.1. BO photoreceptors differentiate in the absence of the apical crb protein complex

As described in previous works (Green et al., 1993) larval PRC precursors, expressing neural markers like the Futsch epitope recognized by the 22C10 antibody (Fujita et al., 1982; Hummel et al., 2000), arise within the bottom part of the optic lobe placode as it invaginates from the head ectoderm during embryonic stage 12 and 13 (Steller et al., 1987; Hartenstein, 1988; Green et al., 1993, Fig. 2A). During this early, epithelial phase of their existence, PRC precursors express the Crb protein at their apical membrane, similar to other sensory neuronal precursors and surrounding epidermal precursors (Fig. 2B, green arrow). The *zonula adherens*, marked by high levels of Arm/β-catenin, forms a belt just basal to the Crb-positive domain (Fig. 2F, yellow arrow). Subsequently, during later stage 13 and stage 14, PRCs segregate from the surface ectoderm (Fig. 2A, C, H) and, following head involution, end up at the basal surface of the dorsal pouch (Fig. 2A). Following internalization, PRC precursors lose or strongly downregulate Crb and Arm expression to a level that cannot be distinguished from background (Fig. 2C, D, H). This contrasts the continued expression of these proteins in adult PRC development (Tepass and Harris, 2007). It also contrasts the behavior of these proteins in other sensory neurons, adult and larva alike, such as those forming the antennal maxillary sensory complex. These cells develop elongated, apical dendrites which, at the transition between inner and outer dendritic segment, are surrounded by a dense cuff of Crb and Arm protein, reflecting the location of the *zonula adherens* and apically adjacent membrane domain (Tepass and Hartenstein, 1994; Hong et al., 2001, Fig. 2C, D, G). Expression of Crb and markers for the zonula adherens remain absent from larval PRCs throughout larval stages (data not shown).

We followed the expression of proteins that form part of the centrioles, including Pericentrin-like protein [PLP; Martinez-Campos et al., 2004) and Asterless (Asl; Varmark et al., 2007; Novak et al., 2014). In postmitotic sensory neurons centrioles transform into the basal bodies

which organize the axonemes of outer dendritic segments (Ishikawa and Marshall, 2011). Accordingly, Asl-positive centrioles/basal bodies can be observed in sensory neuron precursors, including PRC precursors, at embryonic stages 13 and 14 (Fig. 2I–K). From late embryonic stages onward, Asl-positive basal bodies form a hallmark of bipolar sensory neurons, exemplified by the antennal and maxillary complex in Fig.2L, but are absent in PRC precursors of the Bolwig organ (Fig.2L).

3.2. BO photoreceptors form microvillar-like processes at their expanded apical pole

The *Drosophila* BO contains between 10 and 16 photoreceptors which are divided into a smaller population of four primary PRCs that express the rhodopsin Rh5, and a larger and somewhat variable population of secondary PRCs expressing Rh6 (Sprecher et al., 2007, 2011; Keene et al., 2011). Our data confirm the reported finding that these two groups form coherent clusters, with Rh5-PRCs being located posteriorly and ventrally of the Rh6-PRCs (Sprecher and Desplan, 2008, Fig. 3A–C). As reported previously (Sprecher et al., 2011), axonal projections of the two groups terminate in different domains within the larval optic neuropil (LON), whereby Rh5-PRCs occupy a more proximal domain than Rh6-PRCs (Fig. 3D and E). Confocal microscopy does not resolve details of the structure of PRCs at the early larval stage; in some specimens one can detect an enrichment of the GFP-signal at the side of the PRC membrane that faces away from the dorsal pouch epithelium (henceforth called the outer or apical surface of the PRC; Fig. 3F, arrowhead). In late larvae, labeling of the Rh5 subgroup of cells reveals parallel processes covering the outer surface of the BO (Fig. 3G, arrow).

The serial TEM dataset reveals ultrastructural details of the BO. PRCs are arranged in a spindle shaped cluster flanking the outer (basal) membrane of the dorsal pouch epithelium (dpe in Fig. 4A–E). Cell bodies of PRCs have an oval shape. Their basal poles, facing medially (towards the dorsal pouch epithelium), taper into axons that collect into the Bolwig nerve (BN; Fig. 4A and B). Significantly, we detect a group of seven anterior cells whose axons bundle before reaching the posterior tip of the BO (cells 1–7 in Fig. 4C–F); the bundle is enclosed by a smaller group of four posterior cells with axons emerging more posteriorly (cells 8–11 in Fig. 4C–F). Based on location and axonal emergence we interpret the anterior group as the Rh6-PRCs, and the posterior one as the Rh5-PRCs. Ultrastructural features presented in the following are not noticeably different for Rh5-PRs and Rh6-PRCs.

PRCs have a widened apical surface that emits 10–20 processes called "microvillar-like processes" (MLPs) in the following. MLPs vary widely in length, with a mean of 5.5 μm (s.d. = 2.2; n = 41), and are predominantly oriented along the ventro-anterior to dorso-posterior axis (Fig. 4F1–11, H). MLPs originate at all positions of the apical PR membrane. Typically, processes originating anteriorly point anteriorly, and vice versa (Fig. 4F1–11). Along the dorso-ventral axis, MLPs belonging to an individual PRC neuron are irregularly spaced; in some cases, two neighboring processes extend right next to each other, whereas in others, they can be more than one micron apart (Fig. 4F–H). Altogether, MLPs form a thin layer extending directly along the apical membranes of PRC somata. Due to their length, which often exceeds that of a PRC soma, MLPs of neighboring cells are broadly intermingled (Fig. 4G and H).

3.3. Microvillar-like processes of larval photoreceptors are shaped as unbranched beaded fibers

The detailed reconstruction of individual MLPs revealed that these processes projected from irregularly shaped folds and processes formed by the apical PRC membrane (af in Fig. 5A'). These folds often wrap around a small bundle of passing MLPs (Fig. 5A, A', B, D). Folds then split into two or more cylindrical extensions that continue as MLPs, joining the passing bundles of MLPs of other neurons (Fig. 4H). Like regular microvilli, MLPs are filled with bundles of microfilaments (Fig. 5C, small arrowhead); thicker apical folds and processes also contain arrays of microtubules (Fig. 5C, large arrowhead). Once protruded from the PRC soma or apical fold, MLPs, despite of their often considerable length, do not branch (Fig. 4F, H; Fig. 5F, F').

A further highly characteristic feature of MLPs is their beaded shape. Thus, on a given cross section, MLPs vary in diameter from less than 50 nm [the typical thickness of a microvillus in the adult eye rhabdomere
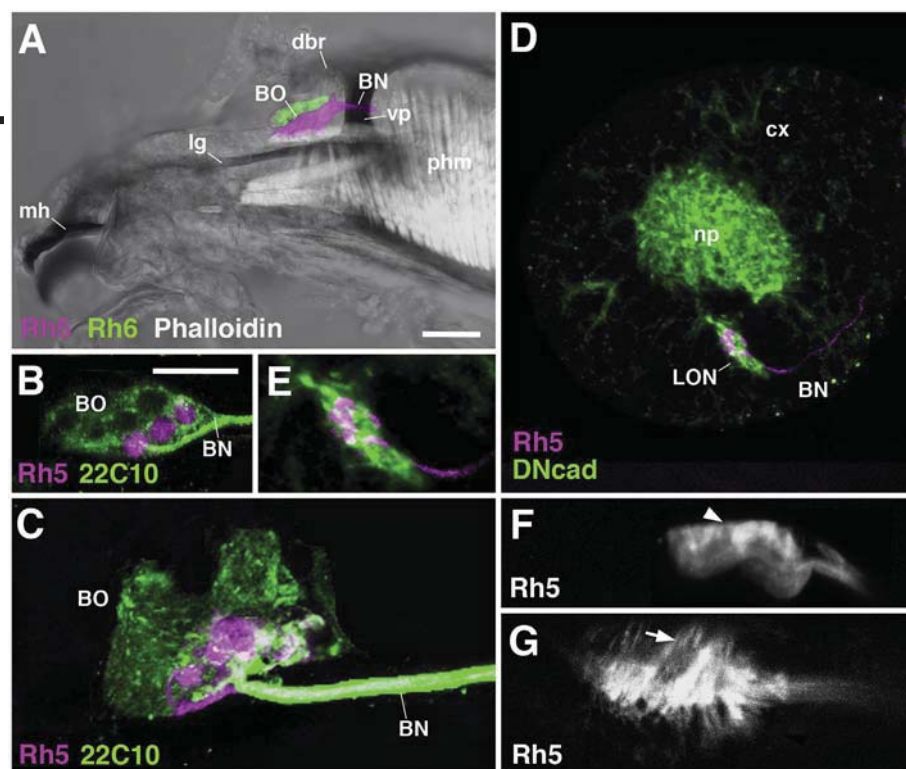
Fig. 3. The larval Bolwig organ. (A) Lateral view of first larval instar head. The two classes of BO neurons expressing Rh5 and Rh6 are labeled by Rh5-Gal4>UAS-mcd8-RFP (magenta) and anti-Rh6 (green), respectively. Pharynx musculature (phm) is labeled by phalloidin (white). Cuticle and cephalopharyngeal skeleton are visible in transmitted light. The Bolwig organ (BO) is situated in the niche formed between the lateralgräten (lg), vertical plate (vp) and dorsal bridge (dbr) of the cephalopharyngeal skeleton. (B, C) Lateral view of Bolwig organ labeled with anti-Futsch (22C10, green) and Rh5-Gal4 (magenta); first instar larva (B) and late third instar larva (C). Note postero-ventral position of Rh5-positive neurons. (D, E) Lateral view of late embryonic brain labeled with anti-DN-cadherin (DNcad, green), showing central brain neuropil (np) and larval optic neuropil (LON). Note projection of Rh5-positive photoreceptors to inner (proximal) domain of LON. (F, G) Rh5 expression in Bolwig organ of first instar larva (F) and late third instar larva (G), revealing apical concentration of signal (arrowhead). In late larva, distinct parallel processes (arrow) traverse the apical surface of the Bolwig organ. Other abbreviations: BN Bolwig nerve; cx brain cortex; mh mouth hooks. Bars: 20 μm (A), 10 μm (B, C, D, F, G).
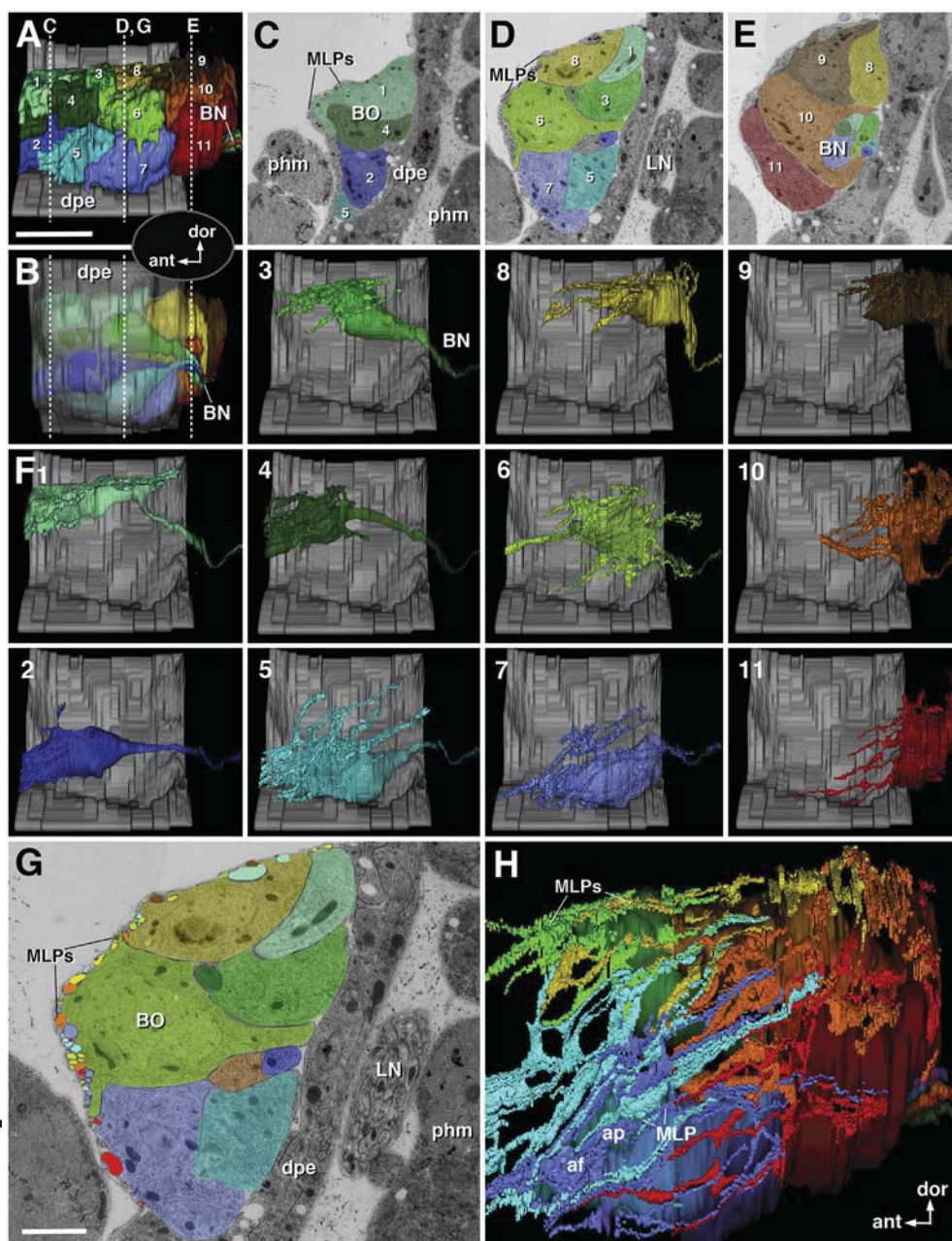
Fig. 4. Serial TEM reconstruction of the Bolwig organ of the first instar larva. (A, B) Digital 3D model of the Bolwig organ in lateral view (A) and medial view (B; anterior to the left, dorsal up). Cell bodies of all photoreceptors are rendered in different colors. Part of the dorsal pouch epithelium (dpe) underlying the Bolwig organ is rendered in grey (semi-transparent in B). (C–E) Electron micrographs of cross sections of Bolwig organ at three different levels (C anterior; D intermediate; E posterior; levels indicated by hatched lines in panels A and B). Cell bodies are shaded in different colors, according to the code used in (A, B). Note that outer (=apical) surface of BO photoreceptors is covered by a thin layer of microvillar-like processes (MLPs). Axons (ax) are given off to the opposite side that flanks the dorsal pouch epithelium (dpe). Also note that in the posterior section (E), axons of the anteriorly located neurons (1–7; see panel F below) have formed a bundle (BN) surrounded by cell bodies of the posterior four BO photoreceptors (8–11), which we interpret to represent the Rh5-positive neurons. (F1-11) Digital 3D models of all 11 Bolwig photoreceptors shown individually in lateral view. Segment of the dorsal pouch epithelium (dpe, in grey) is shown for spatial reference. Microvillar-like processes (MLPs) of irregular length and spacing sprout at different locations from the lateral (presumed apical) membrane of BO photoreceptors. Axons project medially and posteriorly. Note that anterior PRCs (1, 2, 4, 5) are incomplete because their anterior ends were not included in the sectioned block. (G, H) Interdigitation of microvillar-like processes. (G) Presents high magnification of cross section shown in (D), with apically located MLPs rendered in colors corresponding to the cell body of origin. Spatial relationship of MLPs emanating from different cells is also shown in the 3D digital model of subset of BO photoreceptors presented in panel (H). Most frequently, 2–3 processes of the same neuron fasciculate directly adjacent to each other; inbetween these bundled processes, small groups of MLPs of other PRCs extend. Bars: 5 μm (A–F); 2 μm (G, H).

(Hardie and Raghu, 2001); to about 250 nm (Fig. 5B and C). However, following individual MLPs through the series of sections along the z-axis revealed that diameters fluctuated periodically from large to small (Fig. 5E1–10). Thick segments of 0.4–0.8 μm length alternates with approximately equally long thin segments. Many neural processes in the central and peripheral nervous system (e.g., terminal motor axons extending along muscle membranes) have a similar beaded appearance. Here, the beads (="varicosities" or "boutons") often correspond to the site of synapses (Jia et al., 1993; Cardona et al., 2010). In case of the MLPs of photoreceptors, which carry no synapses, the role of the varicosities remains elusive. Only rarely did we observe mitochondria or other organelles filling the varicosities. It is possible that the more or less regularly occurring variations in MLP diameter could represent an emergent property of the elongation of microfilaments, or the interactions of microfilaments with the growing MLP membrane, in the developing larval PRCs.

PRCs of the Bolwig organ are structurally polarized in regard to forming axons and MLPs at roughly opposite cell poles. As described in the previous sections, the MLP-bearing apical cell poles are widened, affording PRCs the shape of an inverted cone (Fig. 6A–D). Ultrastructural features characteristic for the apical pole of rhabdomeric photoreceptors or other epithelial cells, such as the zonula adherens (shown for dorsal pouch epithelium in Fig. 6F, F′, stalk membrane or terminal web are absent. We noted numerous septate junctions interconnecting apical folds and processes of PRCs (Fig. 6F′′, G). A polarized distribution was also observed for Golgi complexes. Each PRC possesses four to six well delineated Golgi complexes (Fig. 5A and B), and in most cases, these were located close to the membrane folds giving rise to MLPs (Fig. 6A–D).

Covering the photoreceptors and MLP layer on its apical surface is a prominent extracellular matrix (ECM; Fig. 6B, C, E). It measured approximately 30 nm in thickness and consists of a thin, dense layer extending parallel to the apical cell surface, and a meshwork of predominantly perpendicularly oriented short fibers. This matrix has the same texture as, and continues uninterruptedly into, the basement
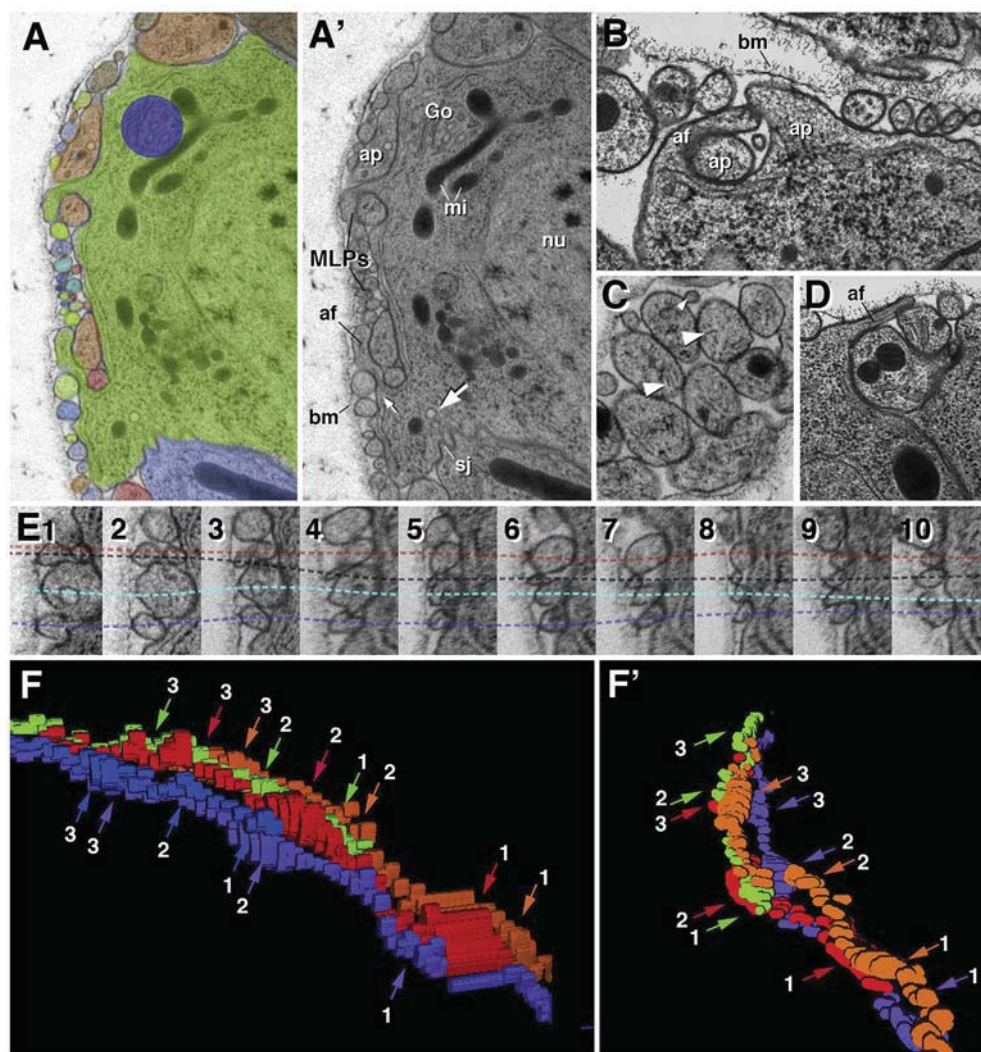
Fig. 5. Ultrastructural features of microvillar-like processes of BO photoreceptors. (A–D) Electron micrographs of sections of apical parts of BO photoreceptors. (A, A′) depict entire apical pole of a cell, showing apical folds (af) and apical processes (ap) that give rise to microvillar-like processes (MLPs). Note prominent Golgi complex (Go) underlying apical membrane, as well as basement membrane (bm) covering layer of MLPs. (B–D) present details of apical membrane shapes (MLPs, apical folds and apical processes at higher magnification. Small arrowhead points at microfilament bundle in thin segment of MLP; large arrowheads indicate microtubule arrays. (E1-10) Series of consecutive sections of bundle of four MLPs. Colored hatched lines follow four individual MLPs. Note alternating increase and decrease in diameter of MLPs. (F) 3D digital model of bundle of MLPs in lateral view (left) and antero-dorsal view (right). Numbered arrows point at segments with larger diameter ("beads") of individual MLPs. Other abbreviations: mi mitochondrium; nu nucleus; sj septate junction. Bars: 1 μm (A, A′); 0.5 μm (B–D); 0.2 μm (E).

membrane covering the basal surface of neighboring dorsal pouch epithelial cells (arrowheads in Fig. 6B).

In their description of a third instar *Drosophila* BO, as well as the late larval PRCs of two representatives of the Muscidae (*Fannia* sp., *Musca domestica*), Melzer and Paulus (1989) characterized the PRC membrane extensions as densely packed lamellae, implying a sheath-like shape for these structures. They also noted that a layer of extracellular matrix ("basal lamina") covered the distal tips of the lamellae. Our third instar larval sections (Green et al., 1993) showed that PRCs give rise to several thick (0.5->1 μm) "stem processes" for which we took over the term "lamellae"; these lamellae further branched into numerous thinner processes with variable diameter and orientation. Compared to the first instar larva, where PRC processes form a thin layer capping the outer surface of the cell bodies (see Fig. 5A), the third instar larva features a BO with a much larger volume that is taken up mostly by the thick stem processes and the large number of thin processes. We speculate that the apical membrane folds seen in the first instar BO (Fig. 5A and B) grow into the stem processes/lamellae of the third instar BO, whereas the thin, cylindrical MLPs increase in number to become the massive population of thin processes.

3.4. Chaoptin is not required for the formation of BO microvillar-like processes

Chaoptin (Chp) was discovered as a membrane glycoprotein expressed by compound eye PRCs throughout development, and required for the normal morphogenesis of these cells (Reinke et al., 1988; Van Vactor et al., 1988). The localization and proper function of Chp depends on the Crb complex (Gurudev et al., 2014). Loss-of-function alleles of *chp*, in adult eyes, result in the virtual absence of rhabdomeres (Van Vactor et al., 1988). Since Chp is expressed in the larval eye (Tomancak et al., 2007) we wondered whether removal of this gene also causes significant abnormalities in the organization of MLPs of BO photoreceptors. Reconstruction of part of a serially sectioned BO of a *chp*-mutant first instar larva demonstrated that MLPs, in the shape of beaded fibers, are still present in abundance (Fig. 7), implying that the relatively sparse and irregular array of BO MLPs (compared to adult rhabdomeres) does not require Chp. Our data do not exclude the possibility that there are quantitative differences in the number and pattern of MLPs in *chp* mutants, but it would require comparison of multiple specimens (of both wild type and mutants) to ascertain such phenotypic differences.

4. Discussion

The main objective of our study was to gain a more detailed knowledge about the three-dimensional structure of larval photoreceptors forming the Bolwig organ. Our results demonstrate that the shape of these cells, in particular in regard to stacking of their apical membranes, differs fundamentally from that observed in adult PRCs. Larval PRCs have a widened apical pole whose membrane is folded into multiple microvillar-like processes that vary in length, diameter, and distance
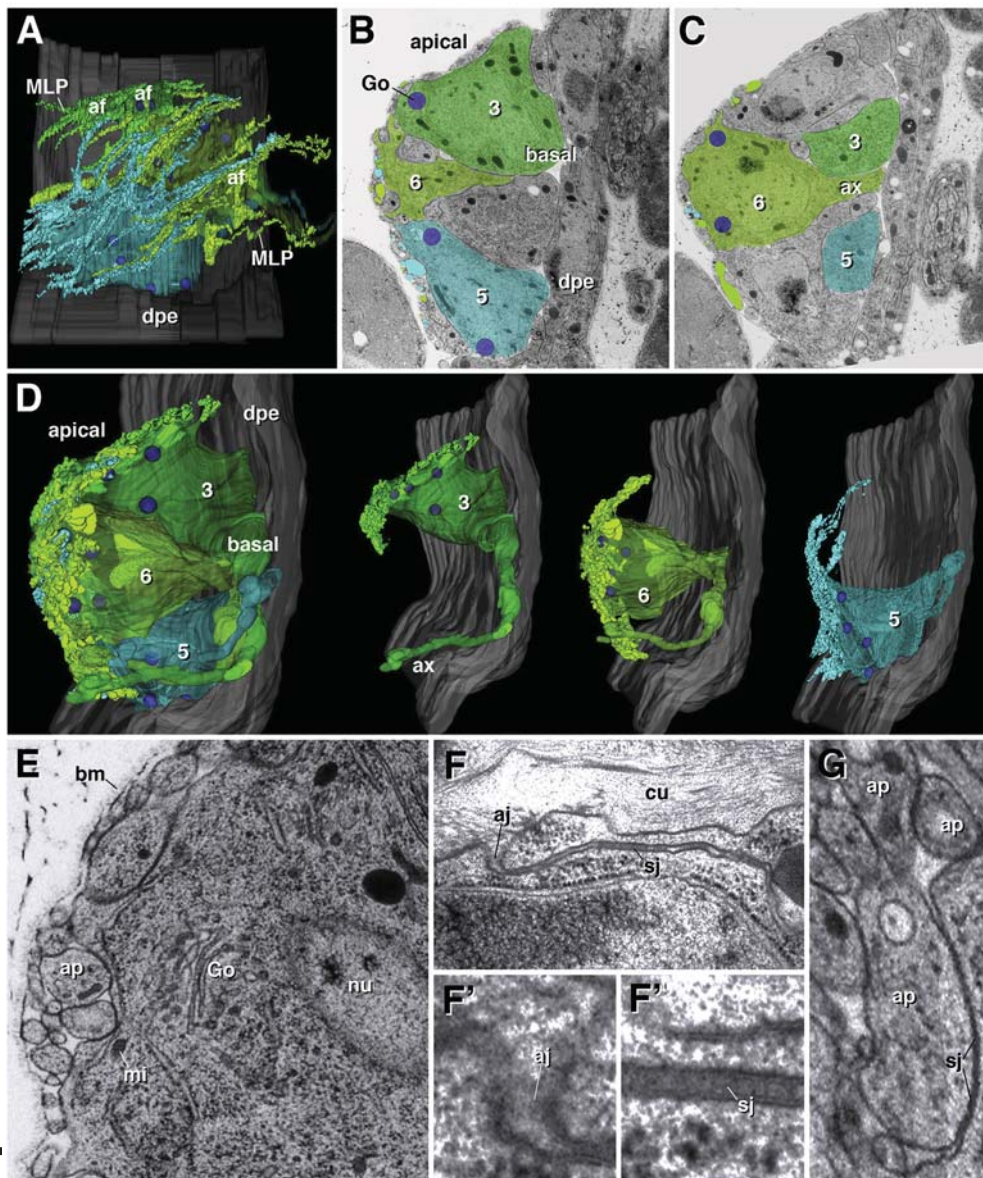
Fig. 6. Apical-basal polarity of BO photoreceptors. (A, B) 3D digital models of three adjacent BO photoreceptors (##3, 5, 6); (A) lateral (=apical) view, (B) posterior view; left in (B): all three PRCs combined; center to right in (B): PRCs shown separately. (C, D) Low power electron micrographs of two sections of Bolwig organ; shapes of PRCs ##3, 5, 6 presented in digital models of (A, B) are shaded in their respective colors. Purple circles in (A–D) outline positions of Golgi apparatus (Go) near apical MLP-bearing membranes of PRCs. (E, E′) Electron micrograph of section of apical pole of PRC illustrating basement membrane (bm). Arrowhead in (E′) indicates dense horizontal layer of basement membrane; arrowhead points at superficial layer consisting of perpendicularly oriented fibers. (F–F″) Apical junctional complex of epithelial cell (dorsal pouch epithelium flanking Bolwig organ), consisting of the *zonula adherens* (a belt-like adherens junction; aj), and septate junctions (sj). (G) Detail of apical membrane processes of PRC which show scattered septate junctions. Other abbreviations: ax axon; Bars: 5 μm (A, D right); 2 μm (B, C, D left); 0.5 μm (E); 0.2 μm (F, G).
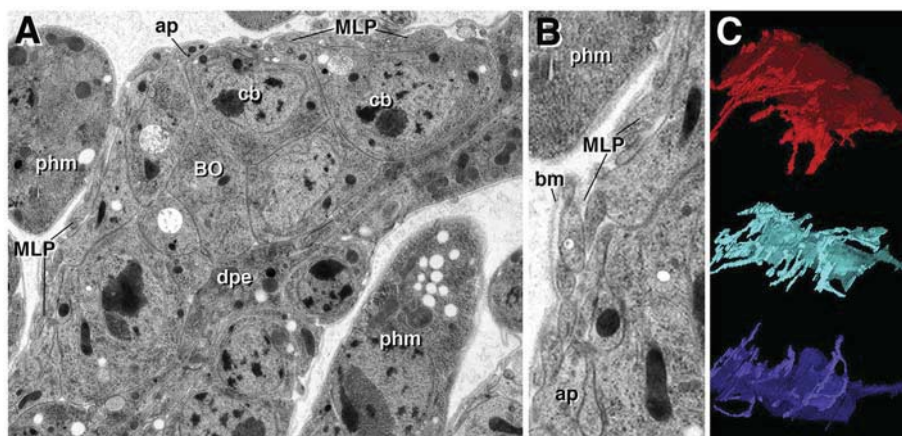
Fig. 7. (A, B) Electron micrographs of BO of first instar larva of *chaoptin* loss-of-function mutant. Features of wild-type BO, including lateral (=apical) layer of microvillar-like processes (MLPs) and apical proesses (ap), covered by basement membrane (bm), are preserved. (C) 3D digital model of three representative PRCs reconstructed from serial TEM of *chp* mutant. Bars: 5 μm (A, C); 0.5 μm (B).

between each other. Unlike microvilli of the adult PRCs' rhabdomeres, which extend from the apical membrane at a perfectly right angle, larval MLPs run more or less parallel to the apical membrane, frequently lying embedded in grooves or folds of this membrane. We surmise that both membrane folds and MLPs increase in size and number between first and third larval instar, resulting in the large membrane "lamellae" that fill out a substantial volume in the late larva (Green et al., 1993; Melzer and Paulus, 1989). What has to be considered as another highly unusual feature of the larval PRCs is the presence of an extracellular matrix, formed by the basement membrane that covers the basal surfaces of neighboring epithelial cells and muscle fibers, and continues uninterruptedly over the apical surface of the Bolwig organ with its layer of microvillar-like processes. In the following we will discuss the peculiar features of the *Drosophila* larval eye in the context of evolutionary and developmental modifications of photoreceptor morphology.

4.1. Photoreceptor membrane stacking: microvilli and microvillar-like processes in different animal clades

Since the introduction of electron microscopy made it possible to study ultrastructural details of different cell types, much attention has been paid to the observation that PRCs enlarge their photosensitive apical membrane by expanding the number/surface of either cilia (ciliary PRCs) or microvilli [rhabdomeric PRCs; (Eakin, 1965, 1968, 1979; Salvini-Plawen, 1982). The favored hypotheses resulting from continuing research into this subject, espoused for example in Purschke et al. (2006), assumes that PRCs emerged among early metazoans from generic epithelial cells which possess both cilia and microvilli. One line of evolution led from this point of departure to PRCs that enlarged number and length of microvilli, and leaving the ciliary compartment unchanged or even reducing it; alternatively, cilia increased in number and/or surface area (see Fig.10 in Purschke et al., 2006). These evolutionary trends tended to happen in parallel in the same species, given the fact that representative species of many phyla possess both ciliary and rhabdomeric PRCs [e.g., rhabdomeric pigmented ocelli and ciliary unpigmented ocelli in annelids (Arendt et al., 2004; Purschke et al., 2006); rhabdomeric dorsal ocelli and ciliary frontal eye in cephalochordates (Lacalli, 2004)]. Even the same PRC can develop ciliary and rhabdomeric elements, as evidenced by the recent finding of gastropod ocelli whose PRCs possessed microvilli and microvillar-like processes as well as cilia, combined with the rhabdomeric and ciliary photo-transduction cascades (Salvini-Plawen, 2009; Vöcking et al., 2017). By contrast, in some taxa such as vertebrates and arthropods, one type of photoreceptor dominates strongly. Arthropod compound eyes and ocelli are exclusively rhabdomeric; only the basal body that transiently exists in PRC precursors, and sometimes persists in adult PRCs (Gottardo et al., 2016; Home, 1972), is a reminder of the original chimaeric, ciliary plus microvillar, nature of the cell from which PRCs developed.

An interesting aspect of photoreceptor diversity that is less frequently discussed concerns the way by which cilia expand their surface area by forming microvilli, or microvillar-like processes. In many ocelli investigated at the ultrastructural level, for example those of cnidarians, gastropods and echinoderms, microvilli sprout from the basal or lateral sides of an elongated cilium (Eakin, 1962; Vaupel-von Harnack, 1963; Blumer, 1994; Garm et al., 2008; Salvini-Plawen, 2009). In some cases, the ciliary axoneme entirely disappears, leaving only basal body and striated rootlet as a reminder of the (presumed) ciliary origin of the apical PRC process from which microvilli extend. In such cases, the distinction between ciliary vs rhabdomeric PRC maybe purely semantic. Indeed, the PRCs found on the arms of sea stars were originally classified as ciliary by Eakin and colleagues (Eakin, 1965, 1979), whereas more recent authors described them as rhabdomeric, even though they express c-opsin (Ullrich-Lüter et al., 2011). Similarly, PRCs of gastropod ocelli are variably classified as rhabdomeric (despite the presence of basal bodies and rootlets) or ciliary (Salvini-Plawen, 2009; Blumer, 1994).

Where do the microvillar-like processes of *Drosophila* larval PRCs fall into the wide spectrum of apical membrane processes observed among different animal phyla? According to the existing developmental and genetic evidence, larval stemmata observed in holometabolous insects, including *Drosophila*, are homologous to the ommatidia of adult compound eyes, a proposition that has been well documented and discussed in previous works (Paulus, 1986, 1989; Melzer and Paulus, 1989; Friedrich, 2013; Buschbeck, 2014). Microvilli of ommatidial rhabdomeres, including those of larval stemmata described for other species, are of extremely uniform diameter, orientation and high packing density, with neighboring microvilli stacked right next to each other (Arikawa et al., 1990; Hardie and Raghu, 2001; Fain et al., 2010). As further discussed below, adhesion-complexes binding microvilli together that have been originally identified in the intestinal brush border, are likely responsible for the tight stacking of rhabdomeric microvilli. Characteristics of PRC microvilli in taxa other than arthropods are also of highly regular diameter and high packing density. This includes basally branching arthropods, such as onychophorans, as well as various lophotrochozoans, including annelids (Fischer and Brökelmann, 1966; Hermans and Cloney, 1966; Krasne and Lawrence, 1966; Dorsett and Hyde, 1968; Röhlich et al., 1970; Whittle and Golding, 1974; Bok et al., 2017), molluscs (Tonosaki, 1967; Boyle, 1969; Dilly, 1969; Hughes, 1970; Kataoka and Yamamoto, 1981; Howard and Martin, 1984; Blumer, 1994; (Salvini-Plawen, 2009), and platyhelminths (MacRae, 1966; Carpenter et al., 1974; Fournier and Combes, 1978; Lanfranchi et al., 1981; (Eakin and Brandenburger, 1981; Bedini and Lanfranchi, 1990; Sopott-Ehlers, 1991), and deuterostomes (Eakin and Kuda, 1971; Braun and Stach, 2017). PRCs of the *Drosophila* Bolwig organ are strikingly different from this picture, with MLPs spaced apart and of irregular length and diameter. Similar cases of more loosely spaced and irregularly oriented microvilli have been described for PRCs of some species belonging to phylogenetically remote taxa, including cnidarians (Singla, 1974; Toh et al., 1979), some larval molluscs (Blumer, 1998) and larval hemichordates (basal deuterostomes; e.g., Brandenburger et al., 1973; Braun et al., 2015). It is reasonable to assume that microvilli number, length and packing density is related to the requirement for light sensitivity, which may be low for small organisms in which visually guided behavior is restricted to positive or negative phototaxis, or simple light/-dark–controlled reflexes (Nilsson, 2013). One might further speculate that in terms of ultrastructure, the simplified structure of the BO PRCs constitutes an atavism, where a reduced requirement for visual acuity and sensitivity reduced the need for an elaborate system of cell biological mechanisms that "streamlines" the architecture of microvilli into an elaborate rhabdomere. Further insights into the differences between genetic control mechanisms of BO PRCs and adult eye PRCs will be instructive to shed light on the question how BO PRCs "devolved" from canonical ommatidial PRCs.

4.2. Cells of the Drosophila larval eye: developmentally truncated rhabdomeric PRCs?

Among the important questions that remain to be addressed are what developmental and genetic mechanisms are controlling the shapes and patterns of rhabdomeric and ciliary membrane specializations encountered in the PRCs of different types of eyes. One plausible interpretation of the peculiar structure of the *Drosophila* larval photoreceptors is that they start out on, and initially follow, a "regular" pathway of rhabdomeric PRC development, but are arrested prematurely. In line with this idea it has been proposed that larval eyes (stemmata) of holometabolous insects are formed by the first groups of cells differentiating at the posterior fringe of the eye field from which the adult compound eye develops (Paulus, 1986; Friedrich, 2003). Genetic investigations in *Drosophila* also reveal fundamental similarities in regard to signaling pathways and transcriptional regulators controlling adult and larval PRC development. The initial step of this process involves the Hedgehog (Hh) and Notch (N) pathways which control the expression of the proneural gene *atonal* (*ato*) in a restricted subset of PRC precursors. In case of the adult eye, these

early specified PRCs are the regularly spaced R8 cells (reviewed in Treisman, 2013); in the BO, they represent the primary photoreceptors, characterized by the expression of the R8-specific opsin Rh5 (Daniel et al., 1999; Chang et al., 2001; Mishra et al., 2018). In a second step, expression of a ligand of EGFR signaling is triggered in the early PRCs, from where it recruits additional PRCs from among the surrounding cells of the eye field. For the adult eye, these cells adopt the fate of the set of R1-6 PCRs (each one defined by a combination of different transcription factors) that surround R8 (Flores et al., 2000). Subsequently, other signaling steps trigger the formation of R7, cone cells and pigment cells. In the BO, the EGFR-recruited cells form a cluster of secondary PRCs that, in terms of photo pigment expressed (Rh6) correspond to R8 cells, rather than R1-6 (Rh1) (Daniel et al., 1999; Mishra et al., 2018). Here we notice the first deviation from the "normal" pathway of PRC specification and ommatidial development: the lack of expression of markers of outer R cells (R1-6), as well as the support cell types (cone cells, pigment cells). This may be linked to another anomaly of the core gene regulatory network of the BO, namely the lack of *ey/Pax 6*. This transcription factor, which plays a central role in specifying PRCs and other elements of they eye in adult flies and most other taxa, is not expressed in precursors of the BO (Daniel et al., 1999; Suzuki and Saigo, 2000).

The differentiation of PRCs begins with their segregation from the epithelial surface, followed by the sprouting of microvilli. In adult eye development, this step takes place in the early pupa, when PRC precursors sink underneath the neighboring quartet of cone cells (Perry, 1968; Cagan and Ready, 1989; Longley and Ready, 1995); in the embryo, BO precursors delaminate from the ectoderm towards the end of stage 13 (Green et al., 1993; see Fig. 2). However, the subsequent events shaping the apical pole of PRCs differs significantly between adult and larval eye. PRCs of the adult eye are still epithelial in character and maintain junctional contacts (*zonula adherens*) and expression of apical and subapical membrane-associated protein complexes, including Crb, DE-cadherin and Arm/β-catenin (Ready and Tepass, 2004; Tepass and Harris, 2007). The tightly connected PRCs of each ommatidium form a small epithelial "vesicle", with their apical membranes constricted and tilted sideways, thereby facing each other (Longley and Ready, 1995). By contrast, BO PRCs, once segregated from the surface, turn down the expression of the apical/subapical protein complexes Crb and Arm/β-catenin. One might speculate that the disappearance of these proteins is controlled at the transcriptional level, by the emergence of larval-specific cis-regulatory elements, as shown recently shown for the proneural gene atonal (Zhou et al., 2017). In the absence of apical markers, like Crb, PLP or Asl, the polarity of BO PRCs is difficult to follow; using the fact that PRC axons mark the basal pole, and interpreting the opposite side of the cell as the apical pole, one can infer that cells rotate, so that the apical pole faces anteriorly during stage 14/15, and comes to point laterally (i.e., 180 deg rotated from the original orientation) by stage 16 (see Fig. 2). However, a clear distinction between apical and basolateral cell surface is not possible.

Beginning at mid-pupal stages, the invaginated apical membranes of adult PRCs sprout microvilli that will form the rhabdomeres. Initially, around 48 h after puparium formation (apf), microvilli directly abut each other, and apical membrane processes are somewhat irregular in diameter and spacing. These early microvilli formed by opposing PRCs interdigitate (Perry, 1968). Soon thereafter, around 50 h apf, apical membranes of PRCs retract, and a lumen, the ommatidial cavity or interommatidial space, forms. Microvilli visible from this stage onward are highly homogenous. When looking at a given PRC, all microvilli are of the same length, diameter and orientation (Perry, 1968; Longley and Ready, 1995; Karagiosis and Ready, 2004; Gurudev et al., 2014). A distinction between rhabdomere (the apical domain carrying microvilli) and stalk membrane (subapical region between rhabdomere and *zonula adherens*) becomes manifest as the ommatidial cavity increases in volume from 55 h apf onward.

The formation of apical microvillar-like processes in the PRCs of the BO takes place in the last hours of embryogenesis. Electron microscopic

studies detailing this process have not yet been conducted, and we therefore don't know whether at an early stage, BO photoreceptor precursors may resemble more closely their adult PRC counterparts. Serial TEM studies on late embryonic heads and brains will shed light on this important question. Given the fact that the apical membrane structure is so radically different between the eyes of adults and larvae (with maintenance of *zonula adherens* and other apical protein complexes, accompanied by apical constriction/invagination only in the former) we consider this possibility as unlikely. What is clear is that at the early larval stage for which the larval eye has been reconstructed in the present study, the structure of apical membrane processes does not resemble the picture presented by adult rhabdomeric microvilli at the mature or any given developmental stage. This finding argues against the interpretation posited hypothetically above, that, in terms of apical membrane structure, BO PRCs merely represent prematurely arrested rhabdomeric (adult) photoreceptors.

4.3. PRC membrane stacking in the absence of crumbs or chaoptin

The rigidly ordered structure of compound eye rhabdomeres has been shown to be regulated by many different molecular pathways, some of them shared with other polarized epithelial cells (including sensory neurons), others expressed uniquely in PRCs. The Crb complex is located around the apical pole of epithelial cells and controls cell polarity and morphogenesis. In PRCs, proteins of this complex shape the apical membrane (stalk membrane vs rhabdomere), and are also essential for the directed transport of additional proteins required for rhabdomeric structure and function (Knust, 2007). The glycoprotein Chaoptin (Chp) was identified as a PRC-specific membrane protein required at different stages of PRC morphogenesis (Reinke et al., 1988); (Van Vactor et al., 1988). During the phase of rhabdomere formation, Chp is crucial for the regular patterning and adhesion of microvilli. In eyes of *chp*-loss-of-function mutants, rhabdomeres are almost missing, and the ommatidial cavity is filled with sparse microvilli of varying length and orientation (Van Vactor et al., 1988), a phenotype that possibly comes close to that of (normal) larval PRCs. In the pupa, rhabdomeric microvilli of *chp*-mutant eyes are more numerous than in the adult mutant, but already irregular in length and orientation. Genetic studies demonstrate that the Crb complex and Chp interact, with the former acting to properly localize the latter (Gurudev et al., 2014).

We speculate that the peculiar structure of larval PRCs of the Bolwig organ can be at least in part attributed to the degradation of the *zonula adherens*, which is manifest once these cells have left the epithelium and become internalized, and to the lack of expression of Crb and, possibly, other polarity proteins playing a role in the elaboration of highly structured rhabdomeres typical for the adult compound eye. Chaoptin expression does appear in the precursors of BO (Tomancak et al., 2007), which may indicate that the *chp* gene employs similar cis-regulatory elements in larval and adult PRC precursors, forming part of a stable cassette of factors that is activated once a cell adopts the photoreceptor fate. However, given the downregulation of Crb and possibly other interacting proteins, Chp may not become properly localized or stabilized. This in conjunction with the spatially unrestrained apical surface of BO PRCs, resulting from the absence of a *zonula adherens*/ommatidial cavity, may be responsible for the small number and irregular pattern of microvillar-like processes formed by larval versus adult PRCs. In the context of such a scenario one could argue that experimental loss of function of the *chp* gene, added to the naturally occurring loss of Crb, does not further enhance the relative "disorganization" of MLPs in the BO, explaining the absence of an overt *chp* mutant phenotype in the early larval BO.

Acknowledgements

References

Salvini-Plawen, von, L., 2009. Photoreception and the polyphyletic evolution of photoreceptors (with special reference to Mollusca)*. doi:10.4003/006.026.0209. https://doi.org/10.4003/006.026.0209, 26, 83–100.

Arendt, D., 2003. Evolution of eyes and photoreceptor cell types. Int. J. Dev. Biol. 47, 563–571.

Arendt, D., Tessmar-Raible, K., Snyman, H., Dorresteijn, A.W., Wittbrodt, J., 2004. Ciliary photoreceptors with a vertebrate-type opsin in an invertebrate brain. Science 306, 869–871. https://doi.org/10.1126/science.1099955.

Arikawa, K., Hicks, J.L., Williams, D.S., 1990. Identification of actin filaments in the rhabdomeral microvilli of Drosophila photoreceptors. J. Cell Biol. 110, 1993–1998.

Bedini, C., Lanfranchi, A., 1990. The eyes of mesostoma ehrenbergi (focke, 1836) (Platyhelminthes, Rhabdocoela). Fine structure and photoreceptor membrane turnover. Acta Zool. 71, 125–133. https://doi.org/10.1111/j.1463-6395.1990.tb01188.x.

Blumer, M., 1994. The ultrastructure of the eyes in the veliger-larvae of Aporrhais sp. and Bittium reticulatum (Mollusca, Caenogastropoda). Zoomorphology 114, 149–159. https://doi.org/10.1007/BF00403262.

Blumer, M.J.F., 1998. Alterations of the eyes of Carinaria lamarcki (Gastropoda, Heteropoda) during the long pelagic cycle. Zoomorphology 118, 183–194. https://doi.org/10.1007/s004350050068.

Bok, M.J., Porter, M.L., Hove, ten, H.A., Smith, R., Nilsson, D.-E., 2017. Radiolar eyes of serpulid worms (Annelida, serpulidae): structures, function, and phototransduction. Biol. Bull. 233, 39–57. https://doi.org/10.1086/694735.

Boyle, P.R., 1969. Fine structure of the eyes of Onithochiton neglectus (Mollusca: polyplacophora). Z. Zellforsch. 102, 313–332.

Brandenburger, J.L., Woollacott, R.M., Eakin, R.M., 1973. Fine structure of eyespots in tornarian larvae (phylum: hemichordata). Z. Zellforsch. 142, 89–102.

Braun, K., Stach, T., 2017. Structure and ultrastructure of eyes and brains of thalia democratica (thaliacea, tunicata, chordata). J. Morphol. 278, 1421–1437. https://doi.org/10.1002/jmor.20722.

Braun, K., Kaul-Strehlow, S., Ullrich-Lüter, E., Stach, T., 2015. Structure and ultrastructure of eyes of tornaria larvae of Glossobalanus marginatus. Org. Divers. Evol. 15, 423–428. https://doi.org/10.1007/s13127-015-0206-x.

Buschbeck, E.K., 2014. Escaping compound eye ancestry: the evolution of single-chamber eyes in holometabolous larvae. J. Exp. Biol. 217, 2818–2824. https://doi.org/10.1242/jeb.085365.

Cagan, R.L., Ready, D.F., 1989. The emergence of order in the Drosophila pupal retina. Dev. Biol. 136, 346–362. https://doi.org/10.1016/0012-1606(89)90261-3.

Cardona, A., Saalfeld, S., Preibisch, S., Schmid, B., Cheng, A., Pulokas, J., Tomancak, P., Hartenstein, V., 2010. An integrated micro- and macroarchitectural analysis of the Drosophila brain by computer-assisted serial section electron microscopy. PLoS Biol. 8, e1000502. https://doi.org/10.1371/journal.pbio.1000502.

Cardona, A., Saalfeld, S., Schindelin, J., Arganda-Carreras, I., Preibisch, S., Longair, M., Tomancak, P., Hartenstein, V., Douglas, R.J., 2012. TrakEM2 software for neural circuit reconstruction. PLoS One 7, e38011. https://doi.org/10.1371/journal.pone.0038011.

Carpenter, K.S., Morita, M., Best, J.B., 1974. Ultrastructure of the photoreceptor of the planarian Dugesia dorotocephala. Cell Tissue Res. 148, 143–158. https://doi.org/10.1007/BF00224579.

Chang, T., Mazotta, J., Dumstrei, K., Dumitrescu, A., Hartenstein, V., 2001. Dpp and Hh signaling in the Drosophila embryonic eye field. Development 128, 4691–4704.

Charlton-Perkins, M., Cook, T.A., 2010. Building a fly eye: terminal differentiation events of the retina, corneal lens, and pigmented epithelia. Curr. Top. Dev. Biol. 93, 129–173. https://doi.org/10.1016/B978-0-12-385044-7.00005-9.

Chou, W.H., Huber, A., Bentrop, J., Schulz, S., Schwab, K., Chadwell, L.V., Paulsen, R., Britt, S.G., 1999. Patterning of the R7 and R8 photoreceptor cells of Drosophila: evidence for induced and default cell-fate specification. Development 126, 607–616.

Daniel, A., Dumstrei, K., Lengyel, J.A., Hartenstein, V., 1999. The control of cell fate in the embryonic visual system by atonal, tailless and EGFR signaling. Development 126, 2945–2954.

Dilly, P.N., 1969. The structure of a photoreceptor organelle in the eye of Pterotrachea mutica. Z. Zellforsch. 99, 420–429. https://doi.org/10.1007/BF00337611.

Dorsett, D.A., Hyde, R., 1968. The fine structure of the lens and photoreceptors of Nereis virens. Z. Zellforsch. 85, 243–255. https://doi.org/10.1007/BF00325039.

Eakin, R.M., 1965. Evolution of photoreceptors. Cold Spring Harbor Symp. Quant. Biol. 30, 363–370. https://doi.org/10.1101/SQB.1965.030.01.036.

Eakin, R.M., 1968. Evolution of photoreceptors. In: Dobzhansky, T., Hecht, M.K., Steere, W.C. (Eds.), Evolutionary Biology. Appleton- Century-Crofts, New York, pp. 194–242.

Eakin, R.M., 1979. Evolutionary significance of photoreceptors: in retrospect. Integr. Comp. Biol. 19, 647–653. https://doi.org/10.1093/icb/19.2.647.

Eakin, R.M., Brandenburger, J.L., 1981. Fine structure of the eyes of Pseudoceros canadensis (Turbellaria, Polycladida). Zoomorphology 98, 1–16. https://doi.org/10.1007/BF00310317.

Eakin, R.M., Kuda, A., 1971. Ultrastructure of sensory receptors in Ascidian tadpoles. Z. Zellforsch. Mikrosk. Anat. 112, 287–312.

Eakin, R.M., Westfall, J.A., 1962. Fine structure of photoreceptors in the hydromedusae, Polyorchis penicillatus. Proc. Natl. Acad. Sci. Unit. States Am. 48, 826–833.

Essen, von, A.M.H.J., Pauls, D., Thum, A.S., Sprecher, S.G., 2011. Capacity of visual classical conditioning in Drosophila larvae. Behav. Neurosci. 125, 921–929. https://doi.org/10.1037/a0025758.

Fain, G.L., Hardie, R., Laughlin, S.B., 2010. Phototransduction and the evolution of photoreceptors. Curr. Biol. 20, R114–R124. https://doi.org/10.1016/j.cub.2009.12.006.

Fan, S.-S., 2004. Dynactin affects extension and assembly of adherens junctions in Drosophila photoreceptor development. J. Biomed. Sci. 11, 362–369. https://doi.org/10.1159/000077105.

Fernald, R.D., 2006. Casting a genetic light on the evolution of eyes. Science 313, 1914–1918. https://doi.org/10.1126/science.1127889.

Fischer, A., Brökelmann, J., 1966. [The eye of Platynereis dumerilii (Polychaeta): its fine structure in ontogenetic and adaptive change]. Z. Zellforsch. Mikrosk. Anat. 71, 217–244.

Flores, G.V., Duan, H., Yan, H., Nagaraj, R., Fu, W., Zou, Y., Noll, M., Banerjee, U., 2000. Combinatorial signaling in the specification of unique cell fates. Cell 103, 75–85.

Fournier, A., Combes, C., 1978. Structure of photoreceptors of Polystoma integerrimum (platyhelminths, monogenea). Zoomorphologie 91, 147–155. https://doi.org/10.1007/BF00993858.

Friedrich, M., 2003. Evolution of insect eye development: first insights from fruit fly, grasshopper and flour beetle. Integr. Comp. Biol. 43, 508–521. https://doi.org/10.1093/icb/43.4.508.

Friedrich, M., 2011. Drosophila as a developmental paradigm of regressive brain evolution: proof of principle in the visual system. Biotechnol. Bioproc. Eng. 78, 199–215. https://doi.org/10.1159/000329850.

Friedrich, M., 2013. Development and evolution of the Drosophila bolwig's organ: a compound eye relict. In: Molecular Genetics of Axial Patterning, Growth and Disease in the Drosophila Eye. Springer, New York, pp. 329–357.

Fujita, S.C., Zipursky, S.L., Benzer, S., Ferrús, A., Shotwell, S.L., 1982. Monoclonal antibodies against the Drosophila nervous system. Proc. Natl. Acad. Sci. U.S.A. 79, 7929–7933.

Garm, A., Andersson, F., Nilsson, D.-E., 2008. Unique structure and optics of the lesser eyes of the box jellyfish Tripedalia cystophora. Vis. Res. 48, 1061–1073. https://doi.org/10.1016/j.visres.2008.01.019.

Gehring, W.J., 2014. The Evolution of Vision, vol. 3. Wiley Interdiscip Rev Dev Biol, pp. 1–40. https://doi.org/10.1002/wdev.96.

Gottardo, M., Callaini, G., Riparbelli, M.G., 2016. Does Unc-GFP uncover ciliary structures in the rhabdomeric eye of Drosophila? J. Cell Sci. 129, 2726–2731. https://doi.org/10.1242/jcs.185942.

Green, P., Hartenstein, A.Y., Hartenstein, V., 1993. The embryonic development of the Drosophila visual system. Cell Tissue Res. 273, 583–598.

Gurudev, N., Yuan, M., Knust, E., 2014. chaoptin, prominin, eyes shut and crumbs form a genetic network controlling the apical compartment of Drosophila photoreceptor cells. Biol Open 3, 332–341. https://doi.org/10.1242/bio.20147310.

Hardie, R.C., Raghu, P., 2001. Visual transduction in Drosophila. Nature 413, 186–193. https://doi.org/10.1038/35093002.

Hartenstein, V., 1988. Development of Drosophila larval sensory organs: spatiotemporal pattern of sensory neurones, peripheral axonal pathways and sensilla differentiation. Development 102, 869–886.

Hermans, C.O., Cloney, R.A., 1966. Fine structure of the prostomial eyes of Armandia brevis (Polychaeta: opheliidae). Z. Zellforsch. 72, 583–596. https://doi.org/10.1007/BF00319262.

Home, E.M., 1972. Centrioles and associated structures in the retinula cells of insect eyes. Tissue Cell 4, 227–234. https://doi.org/10.1016/S0040-8166(72)80044-2.

Hong, Y., Stronach, B., Perrimon, N., Jan, L.Y., Jan, Y.N., 2001. Drosophila Stardust interacts with Crumbs to control polarity of epithelia but not neuroblasts. Nature 414, 634–638. https://doi.org/10.1038/414634a.

Howard, D.R., Martin, G.G., 1984. Fine structure of the eyes of the interstitial gastropod Fartulum orcutti (Gastropoda, Prosobranchia). Zoomorphology 104, 197–203. https://doi.org/10.1007/BF00312031.

Hughes, H.P.I., 1970. A light and electron microscope study of some opisthobranch eyes. Z. Zellforsch. 106, 79–98. https://doi.org/10.1007/BF01027719.

Humberg, T.-H., Sprecher, S.G., 2017. Age- and wavelength-dependency of Drosophila larval phototaxis and behavioral responses to natural lighting conditions. Front. Behav. Neurosci. 11 https://doi.org/10.3389/fnbeh.2017.00066.

Humberg, T.-H., Bruegger, P., Afonso, B., Zlatic, M., Truman, J.W., Gershow, M., Samuel, A., Sprecher, S.G., 2018. Dedicated photoreceptor pathways in Drosophila larvae mediate navigation by processing either spatial or temporal cues. Nat. Commun. 9 https://doi.org/10.1038/s41467-018-03520-5.

Hummel, T., Krukkert, K., Roos, J., Davis, G., Klämbt, C., 2000. Drosophila futsch/22C10 is a MAP1B-like protein required for dendritic and axonal development. Neuron 26, 357–370. https://doi.org/10.1016/S0896-6273(00)81169-1.

Ishikawa, H., Marshall, W.F., 2011. Ciliogenesis: building the cell's antenna. Nature Reviews Molecular Cell Biology 2011 12 (4 12), 222–234. https://doi.org/10.1038/nrm3085.

Izaddoost, S., Nam, S.-C., Bhat, M.A., Bellen, H.J., Choi, K.-W., 2002. Drosophila Crumbs is a positional cue in photoreceptor adherens junctions and rhabdomeres. Nature 416, 178–183. https://doi.org/10.1038/nature720.

Jia, X.X., Gorczyca, M., Budnik, V., 1993. Ultrastructure of neuromuscular junctions in Drosophila: comparison of wild type and mutants with increased excitability. J. Neurobiol. 24, 1025–1044. https://doi.org/10.1002/neu.480240804.

Johnson, K., Grawe, F., Grzeschik, N., Knust, E., 2002. Drosophila crumbs is required to inhibit light-induced photoreceptor degeneration. Curr. Biol. 12, 1675–1680. https://doi.org/10.1016/S0960-9822(02)01180-6.

Justice, E.D., Macedonia, N.J., Hamilton, C., Condron, B., 2012. The simple fly larval visual system can process complex images. Nat. Commun. 3 https://doi.org/10.1038/ncomms2174.

Kane, E.A., Gershow, M., Afonso, B., Larderet, I., Klein, M., Carter, A.R., de Bivort, B.L., Sprecher, S.G., Samuel, A.D.T., 2013. Sensorimotor structure of Drosophila larva phototaxis. Proc. Natl. Acad. Sci. U.S.A. 110, E3868–E3877. https://doi.org/10.1073/pnas.1215295110.

Karagiosis, S.A., Ready, D.F., 2004. Moesin contributes an essential structural role in Drosophila photoreceptor morphogenesis. Development 131, 725–732. https://doi.org/10.1242/dev.00976.

Kataoka, S., Yamamoto, T.Y., 1981. Diurnal changes in the fine structure of photoreceptors in an abalone, Nordotis discus. Cell Tissue Res. 218, 181–189. https://doi.org/10.1007/BF00210103.

Keene, A.C., Sprecher, S.G., 2012. Seeing the light: photobehavior in fruit fly larvae. Trends Neurosci. 35, 104–110. https://doi.org/10.1016/j.tins.2011.11.003.

Keene, A.C., Mazzoni, E.O., Zhen, J., Younger, M.A., Yamaguchi, S., Blau, J., Desplan, C., Sprecher, S.G., 2011. Distinct visual pathways mediate Drosophila larval light avoidance and circadian clock entrainment. J. Neurosci. 31, 6527–6534. https://doi.org/10.1523/JNEUROSCI.6165-10.2011.

Knust, E., 2007. Photoreceptor morphogenesis and retinal degeneration: lessons from Drosophila. Curr. Opin. Neurobiol. 17, 541–547. https://doi.org/10.1016/j.conb.2007.08.001.

Krasne, F.B., Lawrence, P.A., 1966. Structure of the photoreceptors in the compound eyespots of branchiomma vesiculosum. J. Cell Sci. 1, 239–248.

Lacalli, T.C., 2004. Sensory systems in amphioxus: a window on the ancestral chordate condition. Biotechnol. Bioproc. Eng. 64, 148–162. https://doi.org/10.1159/000079744.

Lanfranchi, A., Bedini, C., Ferrero, E., 1981. The ultrastructure of the eyes in larval and adult polyclads (Turbellaria). In: The Biology of the Turbellaria. Springer, Dordrecht, Dordrecht, pp. 267–275. https://doi.org/10.1007/978-94-009-8668-8_35.

Liu, Z., Friedrich, M., 2004. The Tribolium homologue of glass and the evolution of insect larval eyes. Dev. Biol. 269, 36–54. https://doi.org/10.1016/j.ydbio.2004.01.012.

Longley Jr., R.L., Ready, D.F., 1995. Integrins and the development of three-dimensional structure in the Drosophila compound eye. Dev. Biol. 171, 415–433. https://doi.org/10.1006/dbio.1995.1292.

MacRae, E.K., 1966. The fine structure of photoreceptors in a marine flatworm. Z. Zellforsch. 75, 469–484. https://doi.org/10.1007/BF00336876.

Martinez-Campos, M., Basto, R., Baker, J., Kernan, M., Raff, J.W., 2004. The Drosophila pericentrin-like protein is essential for cilia/flagella function, but appears to be dispensable for mitosis. J. Cell Biol. 165, 673–683. https://doi.org/10.1083/jcb.200402130.

Melzer, R.R., Paulus, H.F., 1989. Evolutionary pathways to the larval eyes of insects - higher Dipteran stemmata and the evolutionary development of Bolwig organ. Zeitschrift Fur Zoologische Systematik Und Evolutionsforschung 27, 200–245.

Mishra, A.K., Tsachaki, M., Rister, J., Ng, J., Celik, A., Sprecher, S.G., 2013. Binary cell fate decisions and fate transformation in the Drosophila larval eye. PLoS Genet. 9 https://doi.org/10.1371/journal.pgen.1004027.

Mishra, A.K., Bargmann, B.O.R., Tsachaki, M., Fritsch, C., Sprecher, S.G., 2016. Functional genomics identifies regulators of the phototransduction machinery in the Drosophila larval eye and adult ocelli. Dev. Biol. 410, 164–177. https://doi.org/10.1016/j.ydbio.2015.12.026.

Mishra, A.K., Bernardo-Garcia, F.J., Fritsch, C., Humberg, T.-H., Egger, B., Sprecher, S.G., 2018. Patterning mechanisms diversify neuroepithelial domains in the Drosophila optic placode. PLoS Genet. 14, e1007353. https://doi.org/10.1371/journal.pgen.1007353.

Mollereau, B., Wernet, M.F., Beaufils, P., Killian, D., Pichaud, F., Kühnlein, R., Desplan, C., 2000. A green fluorescent protein enhancer trap screen in Drosophila photoreceptor cells. Mech. Dev. 93, 151–160.

Nilsson, D.-E., 2013. Eye evolution and its functional basis. Vis. Neurosci. 30, 5–20. https://doi.org/10.1017/S0952523813000035.

Novak, Z.A., Conduit, P.T., Wainman, A., Raff, J.W., 2014. Asterless licenses daughter centrioles to duplicate for the first time in Drosophila embryos. Curr. Biol. 24, 1276–1282. https://doi.org/10.1016/j.cub.2014.04.023.

Paulus, H., 1986. Evolutionswege zum Larvalauge der Insekten - ein Modell für die Entstehung und die Ableitung der ozellaren Lateralaugen der Myriapoda von Fazettenaugen. Zool. Jb. Syst. 113, 353–371.

Pellikka, M., Tanentzapf, G., Pinto, M., Smith, C., McGlade, C.J., Ready, D.F., Tepass, U., 2002. Crumbs, the Drosophila homologue of human CRB1/RP12, is essential for photoreceptor morphogenesis. Nature 416, 143–149. https://doi.org/10.1038/nature721.

Perry, M.M., 1968. Further studies on the development of the of Drosophila melanogaster. II. The interommatidial bristles. J. Morphol. 124, 249–262. https://doi.org/10.1002/jmor.1051240209.

Pocha, S.M., Shevchenko, A., Knust, E., 2011. Crumbs regulates rhodopsin transport by interacting with and stabilizing myosin V. J. Cell Biol. 195, 827–838. https://doi.org/10.1083/jcb.201105144.

Purschke, G., Arendt, D., Hausen, H., Müller, M.C.M., 2006. Photoreceptor cells and eyes in Annelida. Arthropod Struct. Dev. 35, 211–230. https://doi.org/10.1016/j.asd.2006.07.005.

Quinn, P.M., Pellissier, L.P., Wijnholds, J., 2017. The CRB1 complex: following the trail of crumbs to a feasible gene therapy strategy. Front. Neurosci. 11, 175. https://doi.org/10.3389/fnins.2017.00175.

Randel, N., Jékely, G., 2016. Phototaxis and the origin of visual eyes. Philos. Trans. R. Soc. Lond. B Biol. Sci. 371, 20150042. https://doi.org/10.1098/rstb.2015.0042.

Ready, D.F., Tepass, U., 2004. Crumbs-dependent epithelial organization in retinal morphogenesis and disease photoreceptor cell biology and inherited retinal degenerations. Rec. Adv. Hum. Biol. 10, 1–20.

Reinke, R., Krantz, D.E., Yen, D., Lawrence Zipursky, S., 1988. Chaoptin, a cell surface glycoprotein required for Drosophila photoreceptor cell morphogenesis, contains a repeat motif found in yeast and human. Cell 52, 291–301. https://doi.org/10.1016/0092-8674(88)90518-1.

Richard, M., Roepman, R., Aartsen, W.M., van Rossum, A.G.S.H., Hollander, den, A.I., Knust, E., Wijnholds, J., Cremers, F.P.M., 2006. Towards understanding CRUMBS function in retinal dystrophies. Hum. Mol. Genet. 15, R235–R243. https://doi.org/10.1093/hmg/ddl195.

Röhlich, P., Aros, B., Virágh, S., 1970. Fine structure of photoreceptor cells in the earthworm, Lumbricus terrestris. Z. Zellforsch. 104, 345–357. https://doi.org/10.1007/BF00335687.

Singla, C.L., 1974. Ocelli of hydromedusae. Cell Tissue Res. 149, 413–429. https://doi.org/10.1007/BF00226774.

Sopott-Ehlers, B., 1991. Comparative morphology of photoreceptors in free-living plathelminths — a survey. Hydrobiologia 227, 231–239. https://doi.org/10.1007/BF00027607.

Sprecher, S.G., Desplan, C., 2008. Switch of rhodopsin expression in terminally differentiated Drosophila sensory neurons. Nature 454, 533–537. https://doi.org/10.1038/nature07062.

Sprecher, S.G., Pichaud, F., Desplan, C., 2007. Adult and larval photoreceptors use different mechanisms to specify the same Rhodopsin fates. Genes Dev. 21, 2182–2195. https://doi.org/10.1101/gad.1565407.

Sprecher, S.G., Cardona, A., Hartenstein, V., 2011. The Drosophila larval visual system: high-resolution analysis of a simple visual neuropil. Dev. Biol. 358, 33–43. https://doi.org/10.1016/j.ydbio.2011.07.006.

Steller, H., Fischbach, K.-F., Rubin, G.M., 1987. disconnected: a locus required for neuronal pathway formation in the visual system of drosophila. Cell 50, 1139–1153. https://doi.org/10.1016/0092-8674(87)90180-2.

Suzuki, T., Saigo, K., 2000. Transcriptional regulation of atonal required for Drosophila larval eye development by concerted action of eyes absent, sine oculis and hedgehog signaling independent of fused kinase and cubitus interruptus. Development 127, 1531–1540.

Tepass, U., Harris, K.P., 2007. Adherens junctions in Drosophila retinal morphogenesis. Trends Cell Biol. 17, 26–35. https://doi.org/10.1016/j.tcb.2006.11.006.

Tepass, U., Hartenstein, V., 1994. The development of cellular junctions in the Drosophila embryo. Dev. Biol. 161, 563–596. https://doi.org/10.1006/dbio.1994.1054.

Toh, Y., Yoshida, M., Tateda, H., 1979. Fine structure of the ocellus of the hydromedusan, Spirocodon saltatrix I. Receptor cells. J. Ultrastruct. Res. 68, 341–352. https://doi.org/10.1016/S0022-5320(79)90166-7.

Tomancak, P., Berman, B.P., Beaton, A., Weiszmann, R., Kwan, E., Hartenstein, V., Celniker, S.E., Rubin, G.M., 2007. Global analysis of patterns of gene expression during Drosophila embryogenesis. Genome Biol. 8, R145. https://doi.org/10.1186/gb-2007-8-7-r145.

Tonosaki, A., 1967. Fine structure of the retina inHaliotis discus. Z. Zellforsch. 79, 469–480. https://doi.org/10.1007/BF00336307.

Treisman, J.E., 2013. Retinal Differentiation in Drosophila, vol. 2. Wiley Interdiscip Rev Dev Biol, pp. 545–557. https://doi.org/10.1002/wdev.100.

Ullrich-Lüter, E.M., Dupont, S., Arboleda, E., Hausen, H., Arnone, M.I., 2011. Unique system of photoreceptors in sea urchin tube feet. Proc. Natl. Acad. Sci. U.S.A. 108, 8367–8372. https://doi.org/10.1073/pnas.1018495108.

Van Vactor, D., Krantz, D.E., Reinke, R., Zipursky, S.L., 1988. Analysis of mutants in chaoptin, a photoreceptor cell-specific glycoprotein in Drosophila, reveals its role in cellular morphogenesis. Cell 52, 281–290.

Varmark, H., Llamazares, S., Rebollo, E., Lange, B., Reina, J., Schwarz, H., Gonzalez, C., 2007. Asterless is a centriolar protein required for centrosome function and embryo development in Drosophila. Curr. Biol. 17, 1735–1745. https://doi.org/10.1016/j.cub.2007.09.031.

Vasiliauskas, D., Mazzoni, E.O., Sprecher, S.G., Brodetskiy, K., Johnston, R.J.J., Lidder, P., Vogt, N., Celik, A., Desplan, C., 2011. Feedback from rhodopsin controls rhodopsin exclusion in Drosophila photoreceptors. Nature 479, 108. https://doi.org/10.1038/nature10451.

Vaupel-von Harnack, M., 1963. On the fine structure of the nervous system of the starfish (Asterias rubens L.). III. The structure of the ocular cushion]. Z. Zellforsch. Mikrosk. Anat. 60, 432–451.

Vöcking, O., Kourtesis, I., Tumu, S.C., Hausen, H., 2017. Co-expression of xenopsin and rhabdomeric opsin in photoreceptors bearing microvilli and cilia. Elife 6. https://doi.org/10.7554/eLife.23435.

Whittle, A.C., Golding, D.W., 1974. The fine structure of prostomial photoreceptors in Eulalia viridis (Polychaeta; Annelida). Cell Tissue Res. 154, 379–398.

Zhou, Q., Yu, L., Friedrich, M., Pignoni, F., 2017. Distinct regulation of atonal in a visual organ of Drosophila: organ-specific enhancer and lack of autoregulation in the larval eye. Dev. Biol. 421, 67–76. https://doi.org/10.1016/j.ydbio.2016.09.023.